# Rapid Heating of Gas/Small Particle Mixture

**K. Y. Wang**[1]
Solar Energy Research Institute,
Golden, CO 80401

**W. W. Yuen**
Department of Mechanical and Environmental Engineering,
University of California,
Santa Barbara, CA 93106

*The concept of using a mixture of particles and air as a medium to absorb radiative energy has been proposed for various applications. In this paper, carbon particles mixed with gas form a medium that absorbs radiation from sources such as concentrated solar energy. A single-particle, two-temperature model is used to study the transient temperature of the particle/gas mixture as it undergoes a constant pressure expansion process. The results indicate that for particles smaller than 1 μm in diameter, the surrounding air can be heated as quickly as the particles, while for particles larger than 1 mm in diameter, the air temperature stays relatively unchanged and the particles are heated to a very high temperature. The scattering albedos from the particles are also calculated, revealing that their contribution from scattering to the heating process is insignificant for particles with diameter less than 1 μm.*

## Introduction

The study of heat transfer for a mixture of particles and gas has been of interest in areas such as airborne aerosol in pollution problems, particle formation in clouds, fluidized beds in combustion chambers, etc. Hunt (1978) proposed the concept of using small particles suspended in a gas to directly absorb solar energy in a cavity for power generation. A later work (Hunt and Brown, 1983) demonstrated in a field test that air temperatures of about 750°C can be achieved when a mixture of air and 0.1-μm-diameter carbon particles are blown through a focal point with 30-kW solar input. More recently, Hruby and Steele (1985) studied the fundamental characteristics of a solid-particle receiver with intensive radiation input. The free-falling particles with sizes ranging from 300 to 1000 μm were observed to achieve a temperature rise of more than 1000°C in a distance about 10 m and a power density of 0.5 MW/m$^2$. The particle temperature was measured by thermocouples inserted into an insulated bucket that collects particles. The basic concept of a solid-particle receiver is illustrated in Fig. 1.

The purpose of the present study is to quantify the thermal performance of such a particle/gas mixture as a function of system parameters such as particle size, density, and flux level. Particular interest is paid to study the maximum gas heating rate. In contrast to many existing works (Houf and Greif, 1985, Evans et al., 1985) which consider only the steady state phenomenon, the present work analyzes the transient heat transfer characteristics of the mixture. Specifically, results of the present work illustrate that a small particle/gas mixture has a unique characteristic that it can achieve an extremely fast rate of temperature increase under direct radiant heating. This characteristic is extremely important in many current applications of small particle/gas mixture in which a chemically reactive mixture is used as a working fluid for direct solar energy conversion (Hunt et al., 1985).

## Analysis

The physical configuration of the system under consideration is shown in Fig. 2. A single-direction, uniformly distributed radiation source with intensity $Q_i$ is incident on a cloud of particles. It is assumed that the particles are uniformly suspended in the gas phase and have an average diameter $d_p$. The characteristic dimension of the cloud is $d_c$, and $d_c >> d_p$. The particles are far apart from each other (typical solid volume fraction $f_v << 1$), and the effects of cloud emission on the energy balance of a single particle is neglected. An analysis which supports the validity of this assumption is presented in the Appendix. To further simplify the analysis, the convective heat transfer due to the relative motions between particles and gas are not considered. The present model is thus valid for a cloud of particles in which the particles are stationary relative to the gas. Similar to Yuen et al. (1986),

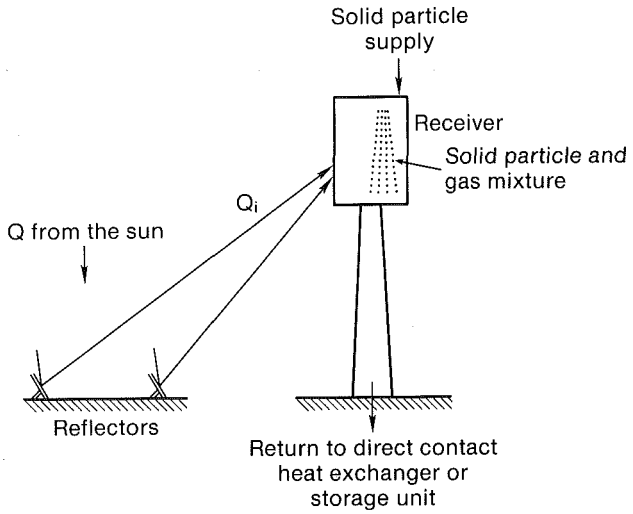


**Fig. 1 Solid-particle solar central receiver**

[1]Present address: Corporate Research and Development, General Electric Company, Schenectady, NY 12345.

Contributed by the Solar Energy Division for publication in the JOURNAL OF SOLAR ENERGY ENGINEERING. Manuscript received by the Solar Energy Division, December, 1985.

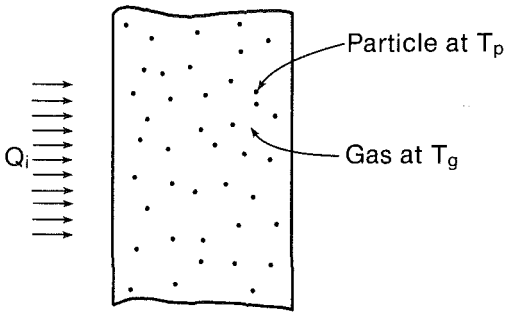


**Fig. 2 Physical configuration of the gas and particle mixture receiving radiative input**

each particle is considered to be surrounded by an adiabatic unit-cell of gas with diameter $d_p/f_v$.

A two-temperature model is adapted to analyze the thermal performance of the mixture. It is assumed that both the gas and the particles are at separate temperatures, yet temperature variation in either phase is neglected. The governing equation for the temperature in gas phase $T_g$ is

$$\rho_g c_g \frac{dT_g}{dt} = \frac{6h}{d_p} \frac{f_v}{1-f_v} (T_p - T_g), \tag{1}$$

and the governing equation for the temperature in the solid phase $T_p$ is

$$\rho_p c_p \frac{dT_p}{dt} = \frac{6h}{d_p} (T_g - T_p) - \frac{1}{f_v} q_R. \tag{2}$$

In equations (1) and (2), $h$ is the heat transfer coefficient which is due only to the conductive heat exchange between the particle and the gas. Since the particle is assumed to be stationary relative to the gas, and the gas expands as it is heated, the solid volume fraction $f_v$ is a function of temperature. As the mixture is heated under a constant pressure condition, $f_v$ can be expressed as

$$f_v = \frac{G}{\rho_p} \frac{T_g(t=0)}{T_g(t)}, \tag{3}$$

where $G$ is the initial mass loading of the mixture, defined as the ratio of total solid mass to total mixture volume, and $\rho_p$ is the density of the particle. The ideal gas law is utilized in the development of equation (3). To illustrate the heat transfer characteristics, the solid particles are assumed to be carbon in all numerical calculations described in the present work. Their properties (Hunt, 1978, Eckert and Drake, 1973) are

$$\rho_p = 2000 \text{ kg/m}^3$$
$$c_p = 712 \text{ J/gK at } 300 \text{ K}.$$

The properties of air are used to represent those for the gas phase. The radiative energy absorbed and emitted by a particle can be approximated as

$$q_R \sim -\frac{3}{2} \frac{1}{d_p} \alpha_p Q_i f_v + \frac{6}{d_p} \epsilon_p \sigma T_p^4 f_v, \tag{4}$$

where $\alpha_p$ and $\epsilon_p$ are the surface absorptivity and emissivity of the particles and can be determined from the Mie theory for spherical particles (van de Hulst, 1957). As previously mentioned, equation (4) neglects the effect of radiative attenuation in the cloud. Therefore, if the optical thickness of the cloud is large (such as with strong absorption and high particle density), the present model has to be modified to take into consideration the radiation variation along the space coordinate. The initial conditions at $t = 0$ for equations (1) and (2) are

$$T_p = T_g = \text{constant}. \tag{5}$$

Equations (1) and (2) can easily be solved numerically using a finite difference method. The gas temperature $T_g$ can be regrouped by taking the solid temperature $T_p$ from equation (1) and substituting it into equation (2) so that an expression for $T_g$ can be obtained.

In a recent study, Houf and Greif (1985) investigated the radiative transport in a falling sheet of solid particles, similar to the configuration under present investigation. In their analysis, $q_R$ was generated by the solution to the equation of transfer, rather than the simple expression equation (4), and the effects of scatteirng was examined. The thermal interaction between the solid and gas phases, however, was not included. In a similar study, Evans et al. (1985) developed a model to predict the gas/particle flow pattern and heat transfer in a two-dimensional, steady state, solid particle solar central receiver. In these previous studies, the particles under investigation range from 100 to 1000 $\mu$min diameter. Their general conclusions are that smaller particles lead to a greater optical thickness for the mixture, longer residence time for the particle and higher convective loss fraction from the cavity. However, all of these previous analyses emphasized the overall performance of the cavity, and did not discuss the transient behavior. The present analysis examines the problem from another viewpoint, with emphasis on the transient interaction between a stationary particle and the surrounding gas. The important parameters will be identified and their effects will be examined.

## Results and Discussion

The optical properties necessary to calculate the radiative properties of the individual particle are the real and imaginary parts of the complex refractive index. Here, the optical

## Nomenclature

$c$ = specific heat
$d$ = diameter
$e_{b\lambda}$ = black body emissive power
$f_v$ = solid volume fraction
$G$ = mass loading factor at initial temperature
$h$ = heat transfer coefficient
Kn = Knudsen number
$n$ = real part of complex refractive index
Nu = Nusselt number
$q_R$ = radiative energy absorbed by a spherical particle
$Q_{abs}$ = absorption efficiency of a spherical particle
$Q_{sca}$ = scattering efficiency of a spherical particle
$Q_i$ = incoming radiative flux
$r$ = radius; distance from an element in the cloud to the center of the particle
$s$ = distance from an element in the cloud to the surface of the particle
$t$ = time
$T$ = temperature
$y$ = space coordinate along the radiation direction
$\alpha$ = absorptivity; accommmodation coefficient
$\epsilon$ = emissivity
$\kappa$ = imaginary part of complex refractive index
$\rho$ = density
$\sigma$ = Stefan-Boltzmann constant
$\sigma_{abs}$ = adsorption coefficient
$\tau$ = optical thickness of the cloud
$\omega$ = scattering albedo

**Subscripts**

$c$ = cloud containing particles and gas
$g$ = gas phase
$o$ = initial state
$p$ = solid (particle) phase

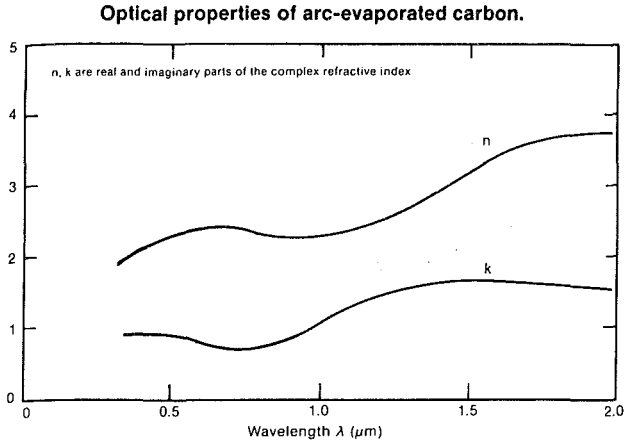


Fig. 3 Optical properties of the carbon particle

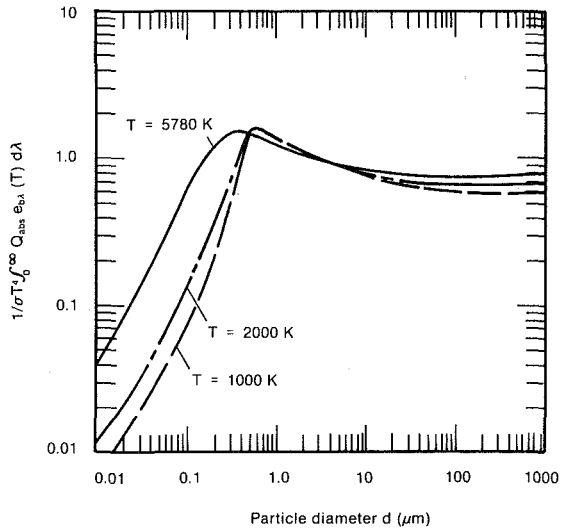


Fig. 4 Radiative characteristics of carbon particles as a function of size

properties of carbon are derived from the results measured by Arakawa et al. (1977) and are plotted in Fig. 3 as a function of wavelength. The Mie scattering theory is then used to calculate the absorption efficiency $Q_{abs}$ of the spherical particle (van de Hulst, 1957). In the case where the particle size is much larger than the wavelength, the so-called geometric optics regime, the relation

$$Q_{abs} = 1 - \left| \frac{n - i\kappa - 1}{n - i\kappa + 1} \right|^2 \tag{6}$$

where $i = \sqrt{-1}$, is used as an approximation to reduce the computing time (Bohren and Hultman, 1983).

To illustrate the characteristics of radiative heat transfer involving small particles, the total absorption efficiency weighted by the black body emission function for the carbon particle is shown in Fig. 4 as a function of particle diameter. The curve for $T = 5780$ K characterizes the absorption of solar radiation by the carbon particle. Similarly, the curves for $T = 1000$ K and 2000 K characterize the emission from the particle at the designated temperatures. It is the ratio of absorption to emission that quantifies the net energy gain for a particle. The results indicate that particles larger than $\sim 1$ $\mu$m have a strong ability to absorb radiation, but also lose energy easily by emission at a lower temperature. On the other hand, the energy absorbed by smaller particles is much greater than

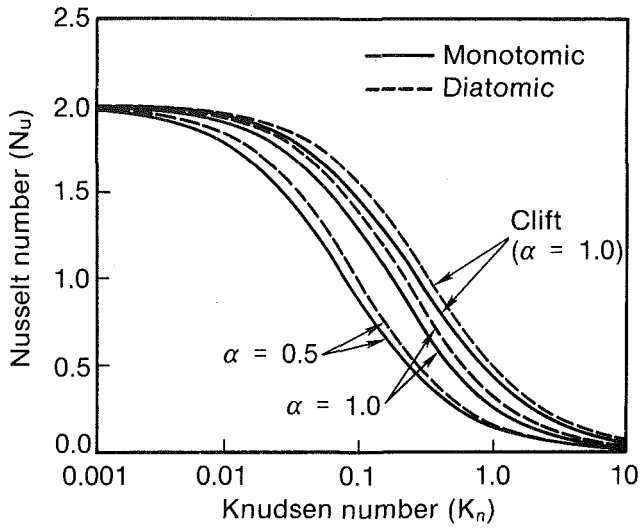


Fig. 5 Nu versus Kn for spherical particles in a motionless gas (Yuen et al., 1984). $\alpha$ is the accommodation coefficient.

that emitted from the particle surface. The equivalent emissivity or absorptivity for a single particle is defined as

$$\epsilon_p(T) \text{ or } \alpha_p(T) = \frac{1}{\sigma T^4} \int_0^\infty Q_{abs} e_{b\lambda}(T) d\lambda, \tag{7}$$

where $e_{b\lambda}$ is the black body emissive power.

In a recent study, Yuen et al. (1984) investigated the rate of heat transfer by conduction from small particles suspended in a gas. The relative motion between the particles and the gas was ignored to simplify the analysis. The study shows that an important dimensionless parameter affecting the heat transfer between a particle and its surrounding gas is the Knudsen number Kn, defined as the ratio of gas molecule mean free path to $d_p$, the particle diameter. The mean free path for air is usually extremely small (e.g., $<0.1$ $\mu$m) in standard temperature and pressure conditions and increases with the absolute temperature. The familiar result for conductive heat transfer between a particle and motionless fluid (Nu = 2) is shown to be accurate only under the condition Kn $<<$ 1.0. However, as the particle size shrinks to be comparable to the gas mean free path, the heat transfer rate reduces since the motions of the gas molecule, which characterize energy transfer by conduction, are hindered. The Nu versus Kn relation for both monotonic and diatomic gas molecules is presented in Fig. 5. Also shown in Fig. 5 is a value of Nu taken from Clift (1978). The variable $\alpha$ is the accommodation coefficient, which is equal to 1 for perfect accommodation (as the temperature of the gas molecule approaches that of the particle), and is equal to 0 if no energy is exchanged.

Utilizing results presented in Figs. 4 and 5, the transient temperature of the solid particles and the gas phase are depicted in Figs. 6(*a*) and 6(*b*), respectively. For small particles (e.g., $d_p < 10^{-5}$m), the heating rate is determined by the net energy gain from direct radiative absorption and emission loss. The temperature between the particles and the gas is extremely small and the energy loss from the particles to the gas is significant in affecting the particle heating rate. For large particles (e.g., $d_p > 10^{-3}$m), the temperature difference between the particle and the gas is quite large. The small surface-area-to-volume ratio makes the energy loss from the particle to the gas quite insignificant in affecting the particle heating rate. The transition from the small particle limit to the large particle limit seems to be between $10^{-5}$ m and $10^{-3}$ m. It is in this transition zone that energy loss from the particle to the gas becomes significant. The relatively slow temperature rise for particles with diameters $10^{-4}$ and $10^{-5}$ m reflects this condi-

Particle temperature of the gas/particle mixture after heated by solar flux Q = $10^6$ W/m². Initial mass loading G = $10^{-3}$ Kg/m³. d is diameter of the particle.

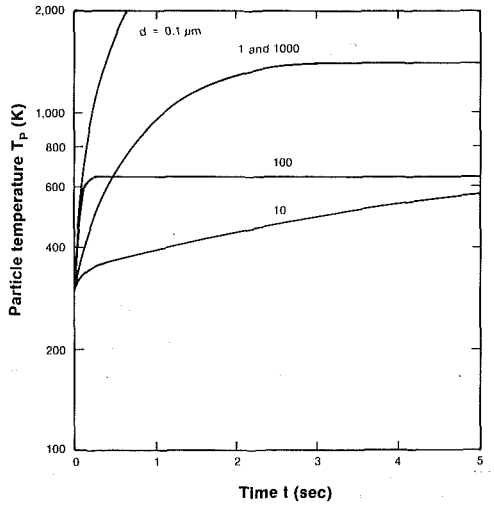


Fig. 6(a) Particle temperature of the mixture after being heated by $Q_i$ = $10^6$ W/m². Initial mass loading G = $10^{-3}$ kg/m³.

Gas temperature of the gas/particle mixture after heated by solar flux Q = $10^6$ W/m². Initial mass loading G = $10^{-3}$ Kg/m³. d is diameter of the particle.

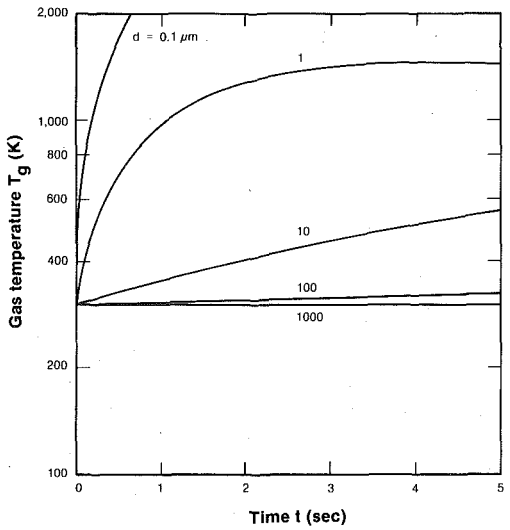


Fig. 6(b) Gas temperature of the mixture after being heated under the same conditions as in 6(a)

tion. It is clear that the highest gas heating rate occurs for a mixture consisting of the smallest particle. This is because the smaller surface-area-to-volume ratio and smaller absorption-to-emission ratio, mentioned above, for the larger particles result in less efficient heat exchange between the solid and gas phases. It is also interesting to note that even in the case of $d_p$ = 1000 $\mu$m, where the gas temperature remains essentially unchanged from the initial state, the solid particles are still very efficient in absorbing radiative energy. A larger-particle/air mixture is thus desirable for a solid-particle solar receiver concept as described by Hruby and Steele (1985), where high-temperature solid particles, not high-temperature air, are the required product. Since the gas and the particle temperatures are almost identical when particles are small enough (e.g., $d_p$ < 1 $\mu$m), a single-temperature model should be acceptable under such circumstances. Adapting this simplification will then allow the model to be extended easily to take into consideration the radiative attenuation in the ray direction which is neglected in this study.

Effect of mass loading G: larger G results in more rapid gas heating, but does not affect the final temperature at steady state.

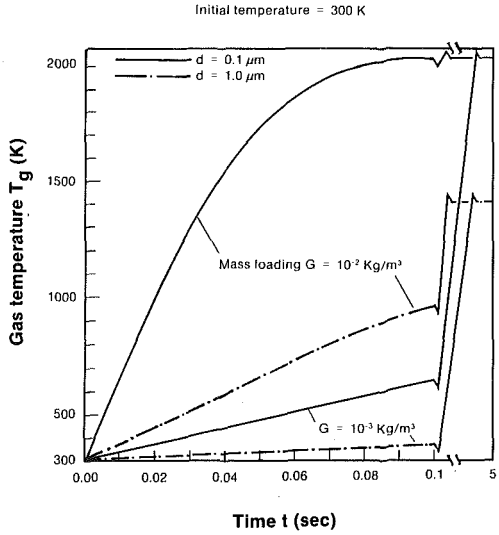


Fig. 7 Effect of mass loading G on gas temperature ($Q_i$ = $10^6$W/m²)

Table 1 Comparison of particle-gas temperature difference between the theoretical limits and the numerical computation

| $d_p$ (μm) | Temperature difference: Theoretical Max. ($T_p - T_g$) (K) | Temperature difference: This work $T_p - T_g$ (K) |
|---|---|---|
| 0.1 | 0.8 | 0 |
| 1 | 2.8 | 0 |
| 10 | 14.1 | 9.7 |
| $10^2$ | 361.1 | 274.4 |
| $10^3$ | 3610.9 | 1093.2 |

The effect of the particle mass loading factor is shown in Fig. 7. It is evident that the amount of solid particles in the mixture strongly affects the rate of radiation absorbed, thus affecting the heating rate of the gas phase. However, it is also interesting to note that the temperature at steady state is not changed by the amount of solid particles in the mixture. The present model, which does not consider the scattering effect and radiative attenuation in the mixture, would not be valid as the optical thickness of the cloud becomes appreciable. The absorption coefficient $\sigma_{abs}$ of the mixture can be expressed as

$$\sigma_{abs} = \frac{3}{2} \frac{Q_{abs}}{d_p} \frac{G}{\rho_p} \frac{T_g(t=0)}{T_g(t)} . \quad (8)$$

Since $\sigma_{abs}$ increases with the mass loading $G$, the validity of the large-mass loading result is somewhat uncertain.

The effect of incoming radiative flux $Q_i$ is shown in Fig. 8. The higher flux renders a higher gas temperature, as expected. However, energy loss by radiation at higher temperature is also higher, and this results in less effective energy gain.

The maximum possible temperature difference between the solid and gas phases has been predicted earlier by Yuen et al. (1986). Using the argument that during the heating process the radiative energy absorbed by the particles is always larger than the conductive energy lost to the surrounding gas, and without considering the emission loss by the particle itself, they concluded that

Table 2 Radiative properties of the carbon particles (weighted by the black body emission power)

| $d_p$(μm) | T = 5780 K | | | T = 2000 K | | | T = 1000 K | | |
|---|---|---|---|---|---|---|---|---|---|
| | $Q_{abs}$ | $Q_{sca}$ | ω | $Q_{abs}$ | $Q_{sca}$ | ω | $Q_{abs}$ | $Q_{sca}$ | ω |
| 0.01 | 0.042 | $1.7 \times 10^{-5}$ | $4.2 \times 10^{-4}$ | 0.012 | $4.8 \times 10^{-7}$ | $4.2 \times 10^{-5}$ | 0.007 | $1.2 \times 10^{-7}$ | $1.7 \times 10^{-5}$ |
| 0.1 | 0.583 | 0.163 | 0.219 | 0.134 | 0.005 | 0.037 | 0.076 | 0.001 | 0.016 |
| 1 | 1.253 | 1.426 | 0.532 | 1.343 | 1.562 | 0.538 | 1.358 | 1.568 | 0.536 |
| 10 | 0.830 | 1.350 | 0.619 | 0.790 | 1.488 | 0.653 | 0.783 | 1.519 | 0.660 |
| 100 | 0.758 | 1.242 | 0.621 | 0.632 | 1.368 | 0.684 | 0.604 | 1.396 | 0.698 |

Table 3 Effect of $h$ on particle and air temperatures

| Nu | h (W/m$^2$ °C) | $T_p$ (K) | $T_g$ (K) |
|---|---|---|---|
| ($d_p = 10^{-7}$m) | | | |
| 2.0 | $2.15 \times 10^6$ | 1750.74 | 1750.70 |
| 1.0 | $1.07 \times 10^6$ | 1750.76 | 1750.68 |
| 0.1 | $1.07 \times 10^5$ | 1751.03 | 1750.24 |
| 0.05* | $5.85 \times 10^4$ | 1751.43 | 1749.98 |
| 0.01 | $1.07 \times 10^4$ | 1751.66 | 1745.80 |
| ($d_p = 10^{-6}$m) | | | |
| 2.0 | $1.02 \times 10^5$ | 682.09 | 679.21 |
| 0.95* | $4.88 \times 10^4$ | 685.12 | 679.05 |
| 0.1 | $5.11 \times 10^3$ | 731.93 | 675.05 |
| 0.01 | $4.48 \times 10^2$ | 1054.54 | 570.27 |
| ($d_p = 10^{-5}$m) | | | |
| 2.0 | $5.58 \times 10^3$ | 363.19 | 326.15 |
| 1.91* | $5.33 \times 10^3$ | 364.92 | 326.16 |
| 1.0 | $2.79 \times 10^3$ | 400.06 | 326.11 |
| 0.1 | $2.75 \times 10^2$ | 944.88 | 321.59 |
| 0.01 | $2.62 \times 10^1$ | 1412.21 | 303.65 |

*Results from Figure 5.

$$T_p - T_g < \frac{Q_i \epsilon_p}{4h} . \tag{10}$$

Their results and the present numerical calculations are listed in Table 1 for comparison. It can be readily observed that the theoretical prediction is satisfactory compared to the numerical results for a small-particle/air mixture. For a large-particle/air mixture the theoretical prediction, although still true, is less accurate.

It was mentioned earlier that the scattering effects are not included in the analysis. The possible contribution from scattering is indicated in Table 2 for different particle sizes. In the table, $Q_{sca}$ is the scattering efficiency of a single sphere and $\omega$ (defined as $Q_{abs}/(Q_{abs} + Q_{sca})$) is the albedo, which is a measure of the relative importance of scattering. It is quite clear that the scattering contribution for very small particles ($d_p < 0.1$ μm) is negligible at low temperatures. Scattering is important and should be included in the analysis for the larger-particle/air mixture. The results shown in Fig. 6(*a*) and Fig. 6(*b*) for the large particle/air mixture can thus be somewhat inaccurate.

The uncertainty in the heat transfer coefficient $h$ is expected to affect the temperatures $T_p$ and $T_g$. This effect is examined and the results are indicated in Table 3. The particle and air temperatures based on Nu from Fig. 5 are shown there, together with results based on arbitrary Nu. It appears that the uncertainty in the Nusselt number for small particles is not significant, as long as the Nusselt number is "large" enough to result in a small difference between the gas and particle temperatures. The range of Nu which renders acceptable results is much larger for small particles than for large ones. As indicated earlier, the Nusselt number obtained in Fig. 5 ignores the relative motion between the particle and the surrounding gas, and this tends to underestimate the heat transfer rate between the two. The calculated values in Table 3 seems to suggest that the errors incurred should be insignificant for particle size as small as $10^{-7}$ m, but may be serious if the particle is larger than $10^{-5}$ m.

Effect of incoming solar flux $Q_{in}$: larger $Q_{in}$ results in higher gas temperature at all times.

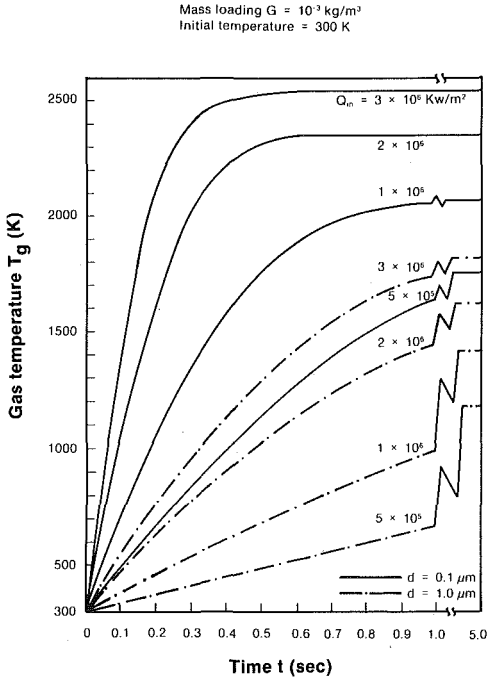


Fig. 8 Effect of incoming radiation flux $Q_i$ on gas temperature ($G = 10^{-3}$ kg/m$^3$)

## Concluding Remarks

This study aims at finding the maximum possible heating rate of the gas phase in a particle/air mixture. A simple two-temperature, transient analysis indicates that very high air temperature (>1000 K) in a very short time (<1 second) appears to be feasible if the particle size, mass loading, and input radiative source are well arranged. Utilizing small particles in a mixture can result in a very high heating rate for the air. However, it should be noted that in the analysis the particle scattering effect, radiation attenuation in the mixture and convective heat transfer between the particle and surrounding gas have been neglected. The consideration of the first two factors tends to lower the gas heating rate while the third factor may render the opposite effect for large particles and gas mixture. Since the temperature difference between the small particle ($d_p < 1$ μm) and the surrounding air is negligible, the present analysis can be modified by adapting a single-temperature model under such circumstances. The simplification will then make transient radiative transfer analyses, such as the two-

flux model or the discrete-ordinate methods, easier to be implemented.

## References


Arakawa, E. T., Williams, M. W., and Inagaki, T., 1977, "Optical Properties of AOC-Evaporated Carbon Films Between 0.6 and 3.8 eV," *Journal of Applied Physics*, Vol. 48, No. 7, pp. 3176-3177.

Bohren, C. F., and Huffman, D. K., 1983, *Absorption and Scattering of Light by Small Particles*, Wiley, New York, p. 172.

Clift, R., 1978, *Bubbles, Drops and Particles*, Academic Press, New York.

Eckert, E. R. G., and Drake, R. M., 1972, *Analysis of Heat and Mass Transfer*, McGraw-Hill, New York.

Evans, G., Houf, W., Greif, R., and Crowe, C., 1985, "Gas-Particle Flow Within Temperature Solar Cavity Receiver Including Radiation Heat Transfer," Heat-Transfer-Denver 1985, Farukhi, N. M., ed., AIChE Symposium Series, No. 245, Vol. 81, pp. 213-219.

Houf, W. G., and Greif, R., 1985, "Radiative Transfer in a Solar Absorbing Particle Laden Flow," presented at the 23rd National Heat Transfer Conference, August 4-7, 1985, Denver, CO.

Hruby, J. M., and Steele, B. R., 1985, "Examination of Solid Particle Central Receiver: Radiant Heat Experiment," *Solar Engineering*, pp. 302-308.

Hunt, A. J., 1978, "Small Particle Heat Exchangers," LBL-7841, Lawrence Berkeley Laboratories, Berkeley, CA.

Hunt, A. J., and Brown, C. T., 1983, "Solar Test Results of an Advanced Direct Absorption High Temperature Gas Receiver," *Proceedings of the 8th Biennial Congress of the International Solar Energy Society*, Vol. 2, Perth, Australia, pp. 959-963.

Hunt, A. J., Ayer, J., Hall, P., Hiller, F., Russo, R., and Tuen, W. W., 1985, "Direct Radiant Heating of Particle Suspensions for the Production of Fuels and Chemicals Using Concentrated Sunlight," LBL-19842, Lawrence Berkeley Laboratory, Berkeley, CA.

van de Hulst, H. C., 1957, *Light Scattering by Small Particles*, Wiley, New York.

Yuen, W. W., Miller, F. J., and Hunt, A. J., 1986, "Heat Transfer Characteristics of Small Particle/Gas Mixture," *International Communication of Heat and Mass Transfer*, Vol. 13, pp. 145-154.

Yuen, W. W., Miller, F. J., and Hunt, A. J., 1984, "A Two-Zone Model for Conduction Heat Transfer from a Particle to a Surrounding Gas at Arbitrary Knudsen Number," LBL-18449, Lawrence Berkeley Laboratories, Berkeley, CA.


## APPENDIX

To illustrate the effect of cloud emission as the energy balance of a single particle within the cloud, consider a particle with radius $r_p$ situated in the middle of a particle cloud with cloud radius $R$. For a mass loading $G$, the particle number density of the cloud can be written as

$$N=\frac{G}{\frac{4}{3}\pi r_p{}^3\rho_p}\left(\frac{T_{g,o}}{T_g}\right) \tag{11}$$

with $T_{g,o}$ being the initial temperature at which the particle cloud is generated and $T_g$ the instantaneous gas temperature. The particles are assumed to be stationary relative to the gas in the development of equation (11). The average inter-particle distance can be written as

$$d_g=2r_g=2\left(\frac{1}{\frac{4}{3}\pi N}\right)^{1/3} \tag{12}$$

Based on equations (11) and (12), the ratio of particle radius to inter-particle radius can be written as

$$\frac{r_p}{r_g}=\left(\frac{GT_{go}}{\rho_p T_g}\right)^{1/3} \tag{13}$$

Note that for most practical applications for which the present work is intended for, $G$ is in the order of $10^{-3}$ Kg/m$^3$ and $\rho_p = 2000$ Kg/m$^3$ for solid carbon. The ratio $r_p/r_g$ is thus typically less than $10^{-2}$.

To estimate the radiative emission from the cloud to a particle, the radiant energy emitted by a differential volume $dV$ to a surface area element $dA_p$ on a particle as shown in Fig. 9 is

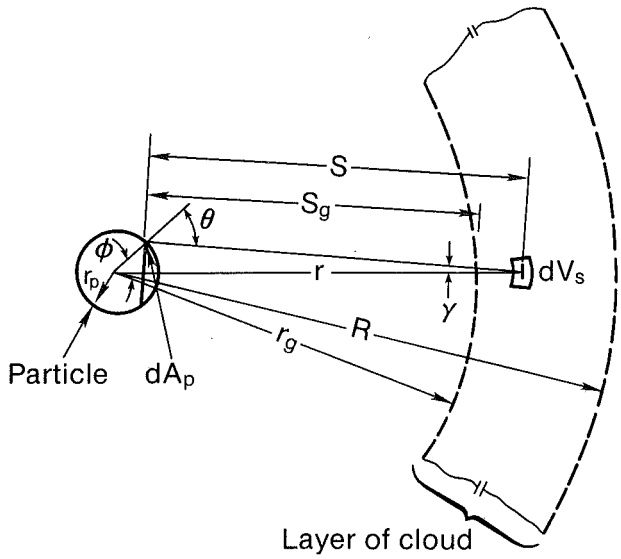


**Fig. 9 Relationship between a particle and the surrounding cloud**

$$dq_R=\sigma_{\text{abs}}\frac{\sigma T_p{}^4}{\pi}\frac{\cos\theta}{s^2}e^{-\tau}dA_p dV_s \tag{14}$$

where $\sigma_{\text{abs}}$ is given by equation (8) and

$$s^2=r^2+r_p{}^2-2rr_p\cos\phi \tag{15}$$

$$dA_p=r_p{}^2\sin\phi d\phi d\gamma \tag{16}$$

$$\theta=\phi+\gamma \tag{17}$$

and $\gamma$ is the azimuthal angle measured relative to the center of the particle. Since the region $r < r_g$ consists only of gas which is assumed to be optically transparent in this work, the optical thickness, $\tau$, is given by

$$\tau=\sigma_{\text{abs}}(s-s_g) \tag{18}$$

Since $r_p/r_g$ is typically less than $10^{-2}$, it can be readily shown that $s_g$ is approximately $r_g$. Equation (18) then becomes,

$$\tau=\sigma_{\text{abs}}(s-r_g) \tag{19}$$

The total radiant energy emitted by $dV$ and intercepted by the whole particle is

$$dq_{R,p}=\sigma_{\text{abs}}dV_s\frac{\sigma T_p^4}{\pi}\int_o^{\cos^{-1}r_p/r}\frac{\cos\theta}{s^2}e^{-\tau}r_p{}^2 2\pi\sin\phi d\phi \tag{20}$$

Since the above expression is independent of the angular coordinate of $dV_s$, the net radiant energy arrived at the particle due to the emission of the surrounding particles can be written as

$$Q_p=\sigma_{\text{abs}}\sigma T_p^4 8\pi r_p{}^2\int_{r_g}^{R}\int_o^{\cos^{-1}\frac{r_p}{r}}\frac{\cos\theta}{s^2}e^{-\tau}r^2\sin\phi d\phi dr \tag{21}$$

Using the fact that $r_p << r_g$, the above integral can be evaluated in closed form to yield

$$Q_p=4\pi r_p{}^2\epsilon(T_g,T_p)\sigma T_p{}^4 \tag{22}$$

where $\epsilon(T_g, T_p)$ can be interpreted as an effective emissivity of the cloud given by

$$\epsilon(T_p,T_g)=1-e-\sigma_{abs}(R-r_g)$$
$$-2\left(\frac{r_p}{r_g}\right)\sigma_{\text{abs}}r_g e^{\sigma_{\text{abs}}r_g}\left[E_1(\sigma_{\text{abs}}r_g)-E_1(\sigma_{\text{abs}}R)\right] \tag{23}$$

where $E_1(x)$ is the familiar exponential integral function defined as

$$E_1(x)=\int_o^1\frac{1}{y}e^{-x/y}dy \tag{24}$$

Based on equation (8) and equation (13), the terms $\sigma_{abs}\, r_g$ can be simplified to yield

$$\sigma_{abs} r_g = \frac{3}{4} Q_{abs} \left(\frac{r_p}{r_g}\right)^3 \tag{25}$$

The cloud radius, $R$, is related to the total number of particles in the cloud, $N_T$, by

$$R = N_T^{1/3} r_g \tag{26}$$

Equations (28) and (26) can be substituted into equation (23) to yield

$$\epsilon(T_p, T_g) = 1 - \exp\left[-\frac{3}{4} (N_T^{1/3} - 1) Q_{abs} (r_p/r_g)^2\right]$$

$$- 1/2 Q_{abs} \left(\frac{r_p}{r_g}\right)^3 \exp\left[\frac{3}{4} Q_{abs} \left(\frac{r_p}{r_g}\right)^2\right] \left[E_1\left(\frac{3}{4}\right.\right.$$

$$\left.\left. Q_{abs} \left(\frac{r_p}{r_g}\right)^2\right) - E_1\left(\frac{3}{4} N_T^{1/3} Q_{abs} \left(\frac{r_p}{r_g}\right)^2\right)\right] \tag{27}$$

Since $r_p/r_g$ is in the order of 0.01 and $Q_{abs}$ is generally in the order of unity, $\epsilon$ $(T_p, T_g)$ is significant only if the product $N_T^{1/3}$ $(r_p/r_g)^2$ is in the order of unity. This requires $N_T$ to be approximately $10^{12}$. The effect of emission by the particle clouds on the energy balance of a single particle is thus insignificant except for an extremely large particle cloud.